Connectivity of the Cognitive Control Network During Response Inhibition as a Predictive and Response Biomarker in Major Depression: Evidence From a Randomized Clinical Trial

Supplementary Information

Table of Contents

Supplemental Methods

Scanning paradigm and preprocessing

Sequence acquisition

The structural dataset was a 3D T1 weighted high resolution SPGR MRI scan, TR = 8.3 ms, TE = 3.2 ms, Flip angle = 11°, TI = 500 ms, NEX = 1, Matrix = 256 × 256, resolution = 1 mm × 1 mm, 180 contiguous 1 mm sagittal slices. Functional data was acquired using an echo planar imaging scan, TR = 2,500 ms, TE = 27.5 ms, Flip angle = 90°, NEX = 1, Matrix = 64 × 64, resolution = 3.75 mm × 3.75 mm, 40 contiguous 3.5 mm axial/oblique slices covering whole brain in each volume; total 120 volumes.

Go-NoGo paradigm

The Go-NoGo paradigm was designed to engage functions of cognitive control (Figure S2). In the NoGo condition, cognitive control was operationalized by withholding behavioral responses to red stimuli (the word "press" in red) relative to a contrast condition of automatic responding to green stimuli (the word "press" in green). The paradigm comprised 60 NoGo stimuli and 180 Go stimuli, presented one at a time in a pseudorandom sequence with a duration of 500 milliseconds and an interstimulus interval of 0.75 seconds. NoGo stimuli were not repeated more than twice in a row. Reaction time and button-box responses were recorded using custom-designed software and hardware.

Preprocessing

fMRI data were preprocessed and analyzed using SPM8 (www.fil.ion.ucl.ac.uk/spm). Unless otherwise specified, default parameters were used. Motion correction was performed by realigning

and unwarping the fMRI images to the first image of each task run. Then, quality control diagnostics were completed on the time-series data for each run. Data volumes that were associated with extreme (*i*) movement (framewise displacement from one time point to the next) and (*ii*) changes in BOLD signal intensity (as indexed by the mean squared difference in signal intensity over the entire volume from one time point to the next divided by the mean signal across the volume averaged across the full time series) were censored (temporally masked) to reduce the influence of motion and related artifacts. Framewise displacement was calculated as the sum of the absolute values of the differentiated realignment estimates as in Power et al. (1). We excluded participants with more than 15% (18) volumes showing frame displacement. For the others, these volumes were censored using established thresholds of framewise displacement ≥0.3 mm and scaled signal intensity differences greater than 10.(1–3) Censoring was implemented with the time-series difference analysis (TSDiffAna) utility (imaging.mrc-cbu.cam.ac.uk/imaging/DataDiagnostics) and in-house scripts. A temporal mask was then created for each censored volume (as well as subsequent volume) and used as regressor of no interest in the first-level statistical models (1, 3). For normalization to stereotactic Montreal Neurological Institute space, the T1-weighted data were normalized to standard space using the FMRIB nonlinear registration tool, and the fMRI EPI data were coregistered to the T1 data using the FMRIB linear registration tool (FMRIB linear registration tool). Normalization warps from these two steps were stored for use in functional-to-standard space transformations. Finally, fMRI data were smoothed using an 8-mm Gaussian kernel, and a high-pass–filter using a cutoff period of 128 seconds was applied.

Within-participant analyses

Contrast map generation for within-participant activation

First-level models were computed for all participants using the onset times of Go and NoGo stimuli convolved with a canonical hemodynamic response function as regressors, and censoring volumes containing movement or artefactual changes in BOLD intensity. Contrast maps for the primary contrast of NoGo>Go were created at pre-treatment baseline and follow-up using one-tailed t-tests. An additional contrast map (the ΔNoGo>Go map) was created for each participant by subtracting the follow-up from the baseline contrast map. These maps were later entered into group-level analyses (see below).

Selection of regions of interest

To assess task-based functional connectivity, we used the generalized psychophysiological interaction (gPPI) toolbox (4). As in the original paper presenting the method, we aimed to select seed regions that showed a BOLD response to the NoGo>Go condition (4). However, previous reports showed differences in activation in MDD compared to HCs (5, 6). Therefore, to ensure selection of comparably active areas in the NoGo>Go condition in *both* MDD participants and HCs, a one-sample t-test was computed within each group using the first-level contrast maps, with age and sex as covariates. Given the high number of subjects and that we were testing within-group effects, we expected the effects for NoGo>Go to be diffuse and larger compared to between-group effects. Therefore, to be able to identify separable clusters of activation, we used a stringent family-wise error (FWE) threshold of $p<0.01$ whole-brain voxel-wise to correct for multiple testing. Only voxels activated in both MDD participants and HCs were selected (Figure S3). We then identified 10 clusters of activation, which required an extent threshold of ≥5 adjacent voxels,

located in gray matter, and within brain boundaries. Spheres with a 6 mm diameter were built around peak voxels of these clusters and were our regions of interest (ROIs) for subsequent connectivity analyses. This yielded 10 ROIs: left postcentral gyrus, right supramarginal gyrus, left orbitofrontal cortex, left external cerebellum, right frontal pole, left globus pallidus and three located in the right middle frontal gyrus (Table S3; see Figure S4 for an illustration of the placement of these ROIs in relation to the original clusters; see Figure S5 for their placement in relation to a meta-analysis of studies on cognitive control). Using the mean signal of spherical ROIs surrounding activation peaks provides reliable values and relatively higher effect sizes compared to other methods, and we chose this approach due to its straightforward implementation and interpretation (7).

Contrast map generation for within-participant functional connectivity

To assess task-based functional connectivity between each ROI and the rest of the brain, we generated first-level models, including an interaction term for each experimental condition obtained by multiplying the stimulus onset regressor convolved with the hemodynamic response function and the ROI timeseries. This approach has a greater sensitivity and specificity than the standard PPI implementation in SPM (4). The contrast of the gPPI terms for NoGo>Go was computed in all participants at baseline and follow-up using a one-sided t-test. As with the activation, we created an additional contrast map for each participant representing the difference between the follow-up and baseline contrast maps ($\Delta NoGo_{gPPI}>Go_{gPPI}$).

Group-level analyses

Our group analyses consisted of two sets of 22 models encompassing each of four participant-level input measures. The first set of models comprised 2-groups t-tests comparing HC and MDD (total tests=22). Depending on the input, these models assessed:

1. NoGo>Go: activation differences at baseline
2. ΔNoGo>Go: difference in activation changes
3. $NoGo_{gPPI}$>Go_{gPPI}: functional connectivity differences at baseline (for each ROI)
4. Δ$NoGo_{gPPI}$>Go_{gPPI}: difference in functional connectivity changes (for each ROI).

We then defined a set of full-factorial models including only MDD. Two factors were used: treatment type (escitalopram, sertraline or venlafaxine-XR) and response (non-responders, responders). First, we tested for an effect of the interaction between the two factors using an F-test to investigate differential response markers between medications (total tests=22). We also compared responders to non-responders within each treatment arm using t-tests (total tests=66). Depending on the input, these tests assessed:

1. NoGo>Go: activation predictors of treatment response
2. ΔNoGo>Go: activation changes related to treatment response
3. $NoGo_{gPPI}$>Go_{gPPI}: functional connectivity predictors of treatment response (for each ROI)
4. Δ$NoGo_{gPPI}$>Go_{gPPI}: functional connectivity changes related to treatment response (for each ROI).

All group-level models included age and sex as covariates of no interest and were masked using a grey matter mask (average of grey matter segmented data from all participants, thresholded at

>0.10 intensity). To detect significant results within each model, a whole-brain uncorrected cluster-forming threshold of $p<0.001$ was set, followed by FWE cluster-level correction at $p<0.05$. Data smoothness was checked for all group-level models using the SPM results window output to assess compatibility with the assumptions of random field theory (8). To account for testing of multiple models, we used two strategies. Our main approach was to apply a second step of FWE correction by multiplying the p_{FWE} cluster-level values of the 18 surviving clusters by 18 and considering as significant only those with resulting $p<0.05$ (p_{FWE} analysis-level). As an alternative approach, we used an experiment-wide correction, and considered significant clusters for which the uncorrected p-value was less than 0.05 divided by the number of group-level tests ($0.05/110=p<0.00045$). When we found functional differences between responders and non-responders, we ran post-hoc Spearman correlations using change in clinical scores across both groups to assess whether results would be applicable regardless of the arbitrary cut-off of 50% symptom reduction to define clinical response.

Predictive models of treatment response

In our gPPI analysis, we found measures of connectivity at baseline that showed an interaction effect between treatment type and response. In particular, coupling between the region pairs dorsolateral prefrontal cortex/supramarginal gyrus and supramarginal gyrus/middle temporal lobe was higher in responders to sertraline and lower in responders to venlafaxine (see Results). To illustrate how these functional markers could be of help in a treatment decision, we ran three classification analyses predicting treatment response. As features, first we used the mean contrast values extracted from the result clusters as two features for each participant treated with sertraline and venlafaxine-XR (Table 2). Then, to assess generalizability of our results to regions

independent from the specific clusters we detected in our participants, we took as reference the neuromorphometrics atlas (http://www.neuromorphometrics.com) and reran our gPPI analyses by using 6 mm diameter spheres centered around the anatomical coordinates of the right middle frontal lobe (which encompassed our dorsolateral prefrontal cortex ROI) and right supramarginal gyrus as ROIs (Table S4). In the same way, we considered as targets spheres around the anatomical centers of the right supramarginal gyrus and right middle temporal lobe. We used the functional connectivity measures between these 2 atlas-based region pairs as predictors for a second classification. Finally, we assessed generalizability of our results to regions consistently activated in cognitive control experiments. We conducted a search on Neurosynth (9) using the term "cognitive control". The resulting map confirmed that our original ROIs are located in regions consistently involved in cognitive control, with the exception of the globus pallidus and orbitofrontal cortex (Figure S5). Then, clusters of the resulting meta-analytic map were identified using FSL's "cluster" tool. Similarly to our primary analysis, we identified clusters greater than 5 voxels and built 6 mm diameter spheres around their activation peak. For one ROI, the activation peak was located on the brain edge and this resulted in a sphere located mostly outside of the brain boundary. Therefore, for this one cluster, the sphere was centered around the center of mass instead of the peak value. Two of the 18 resulting spheres overlapped with our original dorsolateral prefrontal cortex and supramarginal gyrus ROIs. Therefore, we chose these as seeds for a new set of gPPI analyses. As targets, we chose the same supramarginal gyrus ROI and the only Neurosynth-derived sphere located in the middle temporal lobe, although it did not overlap with our results cluster (Table S4).

For each of the three sets of ROIs, we compared a model including only baseline QIDS-SR_{16} (null model) with models including imaging and baseline QIDS-SR_{16}.

Our classifiers were leave-one-out cross-validated logistic regressions in which the optimal regularization parameter lambda was selected as the one returning the minimal error across folds. To build these models, we used the glmnet package in R version 3.5.0. For further optimization, we used nested cross-validation, a procedure in which an inner cross-validation loop is used to perform the tuning of the model parameters while an outer cross-validation loop is used to estimate classification error. This procedure has been shown to significantly reduce bias and give an error estimate that is very close to that obtained on an independent test set (10). Predicted class membership of participants was obtained by binarizing predicted probabilities choosing the threshold maximizing accuracy based on a receiver operating characteristic curve calculated using the R package pROC. Finally, model performance was evaluated by producing a confusion matrix using the caret R package.

Supplemental Results

Experiment-wide family-wise correction for multiple comparisons

When considering significant clusters with an uncorrected p-value<0.00045 (0.05/110), 4 out of our 6 results survived. These were: the interaction effect between treatment type and response for the connectivity between the right DLPFC and right supramarginal gyrus (peak F=14.84, $p_{unc}=6.28*10^{-5}$); the interaction effect between treatment type and response for the coupling between the right supramarginal gyrus and middle temporal gyrus (peak F=19.11, $p_{unc}=3.47*10^{-8}$); the higher functional connectivity in responders to sertraline between the right supramarginal gyrus and the right middle temporal cortex (t=5.33, $p_{unc}=3.97*10^{-5}$); the change in coupling between the left orbitofrontal cortex, left caudate nucleus and brainstem in venlafaxine-XR responders (t=5.16, $p_{unc}=6.01*10^{-6}$). See the main Results for details.

Predictive models of treatment response

In the sertraline arm, baseline QIDS-SR_{16}, was not predictive of treatment response (accuracy 64%, balanced accuracy 63%, sensitivity 53%, specificity 74%, p=0.139). Imaging provided a better classification compared to baseline QIDS-SR_{16} (accuracy 83%, balanced accuracy 84%, sensitivity 95%, specificity 74%, p<0.001). Importantly, these results generalized well to atlas-defined regions independent of our results clusters (QIDS-SR_{16} +imaging model: accuracy 80%, balanced accuracy 81%, sensitivity 67%, specificity 94%, p<0.001). Using Neurosynth-derived ROIs, however, returned an inaccurate classification (QIDS-SR_{16} +imaging model: accuracy 36%, balanced accuracy 38%, sensitivity 63%, specificity 13%, p=0.996).

Performance of models predicting venlafaxine-XR response based on our clusters was slightly lower. QIDS-SR_{16} alone still did not provide a valid classification (accuracy 64%, balanced accuracy 61%, sensitivity 95%, specificity 28%, p=0.130) and was outperformed by QIDS-SR_{16}+imaging (accuracy 77%, balanced accuracy 79%, sensitivity 67%, specificity 89%, p=0.002). Results in the venlafaxine-XR arm, however, did not generalize to anatomically defined regions (accuracy 49%, balanced accuracy 47%, sensitivity 86%, specificity 56%, p=0.789) nor to Neurosynth-derived ROIs (accuracy 15%, balanced accuracy 15%, sensitivity 14%, specificity 17%, p=1).

Detailed performance metrics for all models are shown in Tables S7-S8.

Table S1: Behavioral task performance at baseline.

Resp	HC	Escitalopram			Sertraline			Venlafaxine-XR			HC vs MDD	Treatment
		NR	R	NR vs R	NR	R	NR vs R	NR	R	NR vs R		
N_{BL}	6	19	17		15	20		16	15			
TP_{BL}	180 (179-180)	180 (30-180)	180 (178-180)	U=201.50 p=0.11	180 (20-180)	179 (33-180)	U=105.50 p=0.20	180 (39-180)	180 (145-180)	U=121.50 p=0.71	U=205 p=0.15	KW=2.27 p=0.32
FP_{BL}	6 (3-11)	4.50 (0-29)	3 (1-30)	U=158 p=0.88	4 (0-23)	5 (0-29)	U=182 p=0.18	6 (1-29)	4 (1-16)	U=106.50 p=0.80	U=229.50 p=0.35	KW=0.61 p=0.74
FN_{BL}	0 (0-1)	0 (0-150)	0 (0-2)	U=104 50 p=0.11	0 (0-160)	1 (0-147)	U=179.50 p=0.20	0 (0-141)	0 (0-35)	U=103.50 p=0.71	U=329 p=0.15	KW=2.27 p=0.32
RT mean$_{BL}$	0.30 (0.27-0.41)	0.33 (0.25-0.54)	0.32 (0.21-0.40)	U=131 p=0.48	0.37 (0.26-0.50)	0.33 (0.18-0.58)	U=123 p=0.51	0.34 (0.25-0.46)	0.33 (0.25-0.47)	U=97 p=0.54	U=390 p=0.20	KW=1.88 p=0.39
RT SD$_{BL}$	0.07 (0.05-0.09)	0.08 (0.04-0.18)	0.07 (0.05-0.15)	U=123 p=0.33	0.08 (0.04-0.15)	0.09 (0.05-0.23)	U=168 p=0.39	0.10 (0.04-0.17)	0.07 (0.04-0.14)	U=94 p=0.46	U=398 p=0.16	KW=1.29 p=0.52

Due technical issues, the behavioral data of 53 HC and 22 MDD were lost. We report task performance metrics as median(minimum-maximum). We also report results of statistical tests comparing NR and R within each treatment arm, comparing MDD and HC, assessing differences between treatment arms at baseline. Degrees of freedom for KW=2.

Abbreviations: BL=baseline, FN=false negatives, FP=false positives, HC=healthy controls, KW=Kruskal-Wallis test, MDD=depressed patients, N=number, NR=non-responders, R=responders, RT=reaction time, SD=standard deviation TP=true positives, U=Mann-Whitney U test, XR-extended release.

Table S2: Behavioral task performance at follow-up.

Resp	HC	Escitalopram			Sertraline			Venlafaxine-XR			HC vs MDD	Treatment
		NR	R	NR vs R	NR	R	NR vs R	NR	R	NR vs R		
N_{FU}	4	17	16		16	20		16	10			
TP_{FU}	180 (180-180)	180 (168-180)	180 (175-180)	U=150 p=0.63	180 (43-180)	178.50 (170-180)	U=141.50 p=0.56	180 (173-180)	180 (177-180)	U=73.50 p=0.73	U=108 p=0.17	KW=3.05 p=0.22
FP_{FU}	4 (2-32)	5 (0-27)	4 (1-30)	U=120 p=0.58	2.50 (0-17)	7 (0-23)	U=250.50 p=0.15	6 (0-23)	7 (2-17)	U=116 p=0.86	U=185 p=0.99	KW=1.20 p=0.55
FN_{FU}	0 (0-0)	0 (0-12)	0 (0-5)	U=122 p=0.63	0 (0-137)	1.50 (0-10)	U=178.50 p=0.56	0 (0-7)	0 (0-3)	U=61.50 p=0.73	U=264 p=0.16	KW=3.05 p=0.22
RT $Mean_{FU}$	0.29 (0.19-0.35)	0.32 (0.24-0.44)	0.32 (0.20-0.41)	U=153 p=0.56	0.33 (0.22-0.51)	0.32 (0.19-0.43)	U=148 p=0.72	0.33 (0.24-0.58)	0.31 (0.24-0.44)	U=51 p=0.35	U=244 p=0.31	KW=1.84 p=0.40
RT SD_{FUL}	0.09 (0.03-0.16)	0.07 (0.05-0.28)	0.07 (0.05-0.14)	U=115 p=0.64	0.08 (0.04-0.19)	0.08 (0.05-0.15)	U=188 p=0.39	0.10 (0.04-0.23)	0.07 (0.06-0.11)	U=54 p=0.45	U=164 p=0.73	KW=3.62 p=0.16

Due technical issues, the behavioral data of 55 HC and 29 MDD were lost. We report task performance metrics as median(minimum-maximum). We also report results of statistical tests comparing NR and R within each treatment arm, comparing MDD and HC, assessing differences between treatment arms at follow-up. Degrees of freedom for KW=2.

Abbreviations: FN=false negatives, FP=false positives, FU=follow-up, HC=healthy controls, KW=Kruskal-Wallis test, MDD=depressed patients, N=number, NR=non-responders, R=responders, Resp=response, RT=reaction time, SD=standard deviation TP=true positives, U=Mann-Whitney U test, XR=extended release.

Table S3: ROIs of our gPPI analysis.

Region	Abbreviation	Center (x y z)		
R middle temporal gyrus	MTG	56	-30	-16
R middle frontal gyrus (1)	MFG1	34	58	0
L postcentral gyrus	PCG	-42	-30	46
R supramarginal gyrus	SMG	52	-44	46
L orbitofrontal cortex	OFC	-40	54	-8
L external cerebellum	Cerebellum	-40	-66	-30
R middle frontal gyrus (2)	MFG2	44	24	36
R frontal pole	FP	24	64	-12
R middle frontal gyrus (3)	MFG3	43	20	52
L globus pallidus	GP	-14	-2	-4

We used as regions of interest for our gPPI analysis 6 mm diameter spheres. Reported coordinates are the centers of the spheres in MNI space.

Abbreviations: gPPI=generalized psychophysiological interaction, L=left, MNI=Montreal neurological institute, R=right, ROIs=regions of interest.

Table S4: ROIs and targets of our anatomy- and meta-analysis-based gPPI analysis.

Region	Center (x y z)		
Neuromorphometrics atlas			
Seeds			
R supramarginal gyrus	55.61	-33.36	40.43
R middle frontal gyrus	38.22	31.10	32.41
Targets			
R supramarginal gyrus	55.61	-33.36	40.43
R middle temporal gyrus	59.49	-30.59	-8.30
Neurosynth			
Seeds			
R supramarginal gyrus	52	-46	46
R middle frontal gyrus	36	50	4
Targets			
R supramarginal gyrus	52	-46	46
R middle temporal gyrus	62	-36	-16

We took as reference the neuromorphometrics atlas and reran our gPPI analyses by using as regions of interest and targets 6 mm diameter spheres centered around the coordinates of the regions where we found our results. Then, we conducted a Neurosynth search for the term “cognitive control” and built 6 mm diameter spheres around the resulting activation peaks. We chose as seeds and targets the spheres that overlapped with our results. Reported coordinates are the centers of the spheres in MNI space.

Abbreviations: gPPI=generalized psychophysiological interaction, L=left, MNI=Montreal neurological institute, R=right, ROIs=regions of interest.

Table S5: Generalizability of results to remission and observer clinical rating.

Sertraline arm	**QIDS-SR$_{16}$**	**HRDS$_{17}$**
Responders > Non-responders		
Dorsolateral prefrontal cortex/supramarginal gyrus	**t=4.326, p<0.001**	**t=1.818, p=0.038**
Supramarginal gyrus/middle temporal gyrus	**t=3.591, p=0.001**	**t=1.744, p=0.045**
Supramarginal gyrus/right middle temporal cortex	**t=5.330, p<0.001**	**t=2.250, p=0.015**
Cerebellum/superior temporal gyrus	**t=4.760, p=0.001**	**t=2.647, p=0.006**
Postcentral gyrus/superior temporal gyrus (longitudinal change)	t=4.859, p=0.002	n. s.
Remitters > Non-remitters		
Dorsolateral prefrontal cortex/supramarginal gyrus	t=1.608, p=0.057	n. s.
Supramarginal gyrus/middle temporal gyrus	**t=2.516, p=0.008**	**t=2.705, p=0.004**
Supramarginal gyrus/right middle temporal cortex	**t=2.471, p=0.009**	**t=2.680, p=0.005**
Cerebellum/superior temporal gyrus	**t=3.107, p=0.002**	**t=2.491, p=0.008**
Postcentral gyrus/superior temporal gyrus (longitudinal change)	**t=3.348, p<0.001**	**t=2.147, p=0.019**
Correlation with symptoms improvement		
Dorsolateral prefrontal cortex/supramarginal gyrus	**r=-0.566, p<0.001**	**r=0.351, p=0.012**
Supramarginal gyrus/middle temporal gyrus	**r=-0.560, p<0.001**	**r=-0.473, p=0.001**
Supramarginal gyrus/right middle temporal cortex	**r=-0.527, p<0.001**	**r=-0.364, p=0.009**
Cerebellum/superior temporal gyrus	r=-0.462, p<0.001	n. s.
Postcentral gyrus/superior temporal gyrus (longitudinal change)	**r=0.588, p<0.001**	**r=0.348, p=0.013**
Non-responders > Healthy controls		
Dorsolateral prefrontal cortex/supramarginal gyrus	**t=-3.477, p<0.001**	**t=-2.212, p=0.015**
Supramarginal gyrus/middle temporal gyrus	t=-2.081, p=0.044	n. s.
Supramarginal gyrus/right middle temporal cortex	t=-2.212, p=0.040	n. s.
Cerebellum/superior temporal gyrus	**t=-3.732, p=0.001**	**t=2.182, p=0.018**
Postcentral gyrus/superior temporal gyrus (longitudinal change)	t=-3.066, p=0.004	n. s.
Non-remitters > Healthy controls		
Dorsolateral prefrontal cortex/supramarginal gyrus	**t=-1.984, p=0.025**	**t=-1.734, p=0.043**
Supramarginal gyrus/middle temporal gyrus	n. s.	n. s.
Supramarginal gyrus/right middle temporal cortex	n. s.	n. s.
Cerebellum/superior temporal gyrus	t=-1.947, p=0.027	n. s.
Postcentral gyrus/superior temporal gyrus (longitudinal change)	t=-1.162, p=0.054	n. s.
Responders > Healthy controls		
Supramarginal gyrus/middle temporal gyrus	**t=-4.315, p<0.001**	**t=-2.916, p=0.002**
Supramarginal gyrus/right middle temporal cortex	**t=-3.437, p=0.002**	**t=-3.235, p=0.001**
Cerebellum/superior temporal gyrus	t=-2.524, p=0.015	n. s.
Postcentral gyrus/superior temporal gyrus (longitudinal change)	t=-3.567, p=0.001	n. s.
Remitters > Healthy controls		
Supramarginal gyrus/middle temporal gyrus	n. s.	n. s.
Supramarginal gyrus/right middle temporal cortex	**t=-3.485, p<0.001**	**t=-3.635, p<0.001**
Cerebellum/superior temporal gyrus	**t=-1.815, p=0.037**	**t=-1.630, p=0.053**
Postcentral gyrus/superior temporal gyrus (longitudinal change)	**t=-2.563, p=0.006**	**t=-1.930, p=0.029**

Venlafaxine arm	**QIDS-SR$_{16}$**	**HRDS$_{17}$**
Non-responders > Responders		
Dorsolateral prefrontal cortex/supramarginal gyrus	t=-3.611, p=0.001	n. s.
Supramarginal gyrus/middle temporal gyrus	t=-3.721, p=0.009	n. s.
Non-remitters > Remitters		
Dorsolateral prefrontal cortex/supramarginal gyrus	**t=4.314, p<0.001**	**t=1.722, p=0.046**
Supramarginal gyrus/middle temporal gyrus	**t=3.669, p<0.001**	**t=2.223, p=0.016**
Correlation with symptoms improvement		
Dorsolateral prefrontal cortex/supramarginal gyrus	**r=0.441, p=0.005**	**r=0.294, p=0.001**
Supramarginal gyrus/middle temporal gyrus	**r=0.457, p=0.003**	**r=0.323, p=0.024**
Orbitofrontal cortex/diencephalon (longitudinal change)	**r=-0.658, p<0.001**	**r=-0.284, p=0.042**
Healthy controls > Responders		
Dorsolateral prefrontal cortex/supramarginal gyrus	**t=3.234, p=0.010**	**t=1.667, p=0.049**
Healthy controls > Remitters		
Dorsolateral prefrontal cortex/supramarginal gyrus	**t=3.797, p<0.001**	**t=1.912, p=0.030**
Non-responders > Healthy controls		
Supramarginal gyrus/middle temporal gyrus	t=2.489, p=0.017	n. s.
Non-remitters > Healthy controls		
Supramarginal gyrus/middle temporal gyrus	**t=2.252, p=0.013**	**t=1.753, p=0.042**
Responders > Non-responders		
Orbitofrontal cortex/diencephalon (longitudinal change)	t=5.160, p<0.001	n. s.
Remitters > Non-remitters		
Orbitofrontal cortex/diencephalon (longitudinal change)	t=3.424, p<0.001	n. s.
Responders > Healthy controls		
Orbitofrontal cortex/diencephalon (longitudinal change)	t=3.127, p=0.004	n. s.
Remitters > Healthy controls		
Orbitofrontal cortex/diencephalon (longitudinal change)	t=3.017, p=0.002	n. s.

To test if our results would hold when taking into account an observer-rated scale to define treatment response, we investigated them post-hoc considering treatment response as a ³ 50% decrease in HRSD$_{17}$ instead than in QIDS-SR$_{16}$. Also, we tested if our results would hold when considering remission (QIDS-SR$_{16}$ ≤5 at follow-up or HRDS$_{17}$ ≤7) instead of treatment response. p-values for 2-tailed tests are shown for the original results (QIDS-SR$_{16}$ and clinical response). For tests including HRDS$_{17}$ and remission, p-values are for confirmatory one-tailed tests. Comparisons in bold were significant for both QIDS-SR$_{16}$ and HRSD$_{17}$.

Abbreviations: HRDS$_{17}$=Hamilton Rating Scale for Depression, n. s.=non-significant (p>0.05), QIDS-SR$_{16}$= Quick Inventory of Depressive Symptomatology–Self-Rated.

Table S6: Predictive models of treatment response to sertraline

Performance Metrics	QIDS-SR$_{16}$	QIDS-SR$_{16}$+Imaging		
		Original ROIs & targets	Atlas ROIs & targets	Neurosynth ROIs & targets
Threshold	0.542	0.662	0.388	0.612
Confusion matrix	[10 6 ; 9 17]	[18 6 ; 1 17]	[11 3 ; 8 20]	[12 20 ; 7 3]
Accuracy	0.643	0.833	0.795	0.357
No information rate	0.548	0.548	0.548	0.548
P(accuracy> no information rate)	0.139	<0.001	<0.001	0.995
Sensitivity	0.526	0.947	0.667	0.631
Specificity	0.739	0.739	0.944	0.130
Positive predictive value	0.625	0.750	0.933	0.375
Negative predictive value	0.654	0.944	0.708	0.300
Prevalence	0.452	0.452	0.538	0.452
Detection rate	0.238	0.429	0.359	0.286
Detection prevalence	0.381	0.571	0.385	0.286
Balanced accuracy	0.633	0.843	0.806	0.381

Performance metrics of nested cross-validated logistic regressions predicting response to sertraline using baseline QIDS and the mean functional connectivity contrast values (NoGo>Go) as features. Functional connectivity was extracted respectively from the result clusters of our group comparison as well as from anatomically and Neurosynth-defined gPPI ROIs and targets.

Abbreviations: gPPI=generalized psychophysiological interaction, QIDS-SR$_{16}$=Quick Inventory of Depressive Symptomatology–Self-Rated, ROIs=regions of interest.

Table S7: Predictive models of treatment response to venlafaxine

Performance Metrics	QIDS-SR$_{16}$	QIDS-SR$_{16}$+Imaging		
		Original ROIs & targets	Atlas ROIs & targets	Neurosynth ROIs & targets
Threshold	0.473	0.392	0.436	0.454
Confusion matrix	[20 13 ; 1 5]	[14 2 ; 7 16]	[0 1 ; 21 17]	[3 15 ; 18 3]
Accuracy	0.641	0.769	0.436	0.154
No information rate	0.538	0.538	0.538	0.538
P(accuracy> no information rate)	0.130	0.002	0.926	1
Sensitivity	0.952	0.667	0	0.143
Specificity	0.278	0.889	0.944	0.166
Positive predictive value	0.606	0.875	0	0.166
Negative predictive value	0.833	0.696	0.447	0.142
Prevalence	0.539	0.538	0.538	0.538
Detection rate	0.512	0.359	0	0.077
Detection prevalence	0.846	0.410	0.026	0.461
Balanced accuracy	0.615	0.778	0.472	0.155

Performance metrics of nested cross-validated logistic regressions predicting response to sertraline using baseline QIDS and the mean functional connectivity contrast values (NoGo>Go) as features. Functional connectivity was extracted respectively from the result clusters of our group comparison as well as from anatomically and Neurosynth-defined gPPI ROIs and targets.

Abbreviations: gPPI=generalized psychophysiological interaction, QIDS-SR$_{16}$=Quick Inventory of Depressive Symptomatology–Self-Rated, ROIs=regions of interest.

Table S8: Functional networks of our ROIs and result clusters.

Group contrast	Subject contrast	ROI	ROI network	Results network
Treatment x Response				
	$NoGo_{gPPI}>Go_{gPPI}$	Rt MFG1	Frontoparietal	Ventral attention
	$NoGo_{gPPI}>Go_{gPPI}$	Rt SMG	Frontoparietal	Visual/Dorsal attention
SerR>SerNR				
	$NoGo_{gPPI}>Go_{gPPI}$	Rt SMG	Default mode	Dorsal attention
	$NoGo_{gPPI}>Go_{gPPI}$	Cerebellum	None	Ventral attention
	$\Delta NoGo_{gPPI}>Go_{gPPI}$	L PCG	Dorsal attention	Default mode
VenR>VenNR				
	$\Delta NoGo_{gPPI}>Go_{gPPI}$	L OFC	Frontoparietal	None

We show the location of our gPPI ROIs and results clusters according to known resting state functional connectivity networks as defined by Yeo et al. (11). See also Figures S10-S13.

Abbreviations: gPPI=generalized psycho-physiological interaction, L=left, MFG=middle frontal gyrus, NR=non-responders, OFC=orbitofrontal cortex, PCG=post-central gyrus, R=responders, Rt=right, ROI=region of interest, Ser=sertraline, SMG=supramarginal gyrus.

Figure S1: CONSORT diagram.

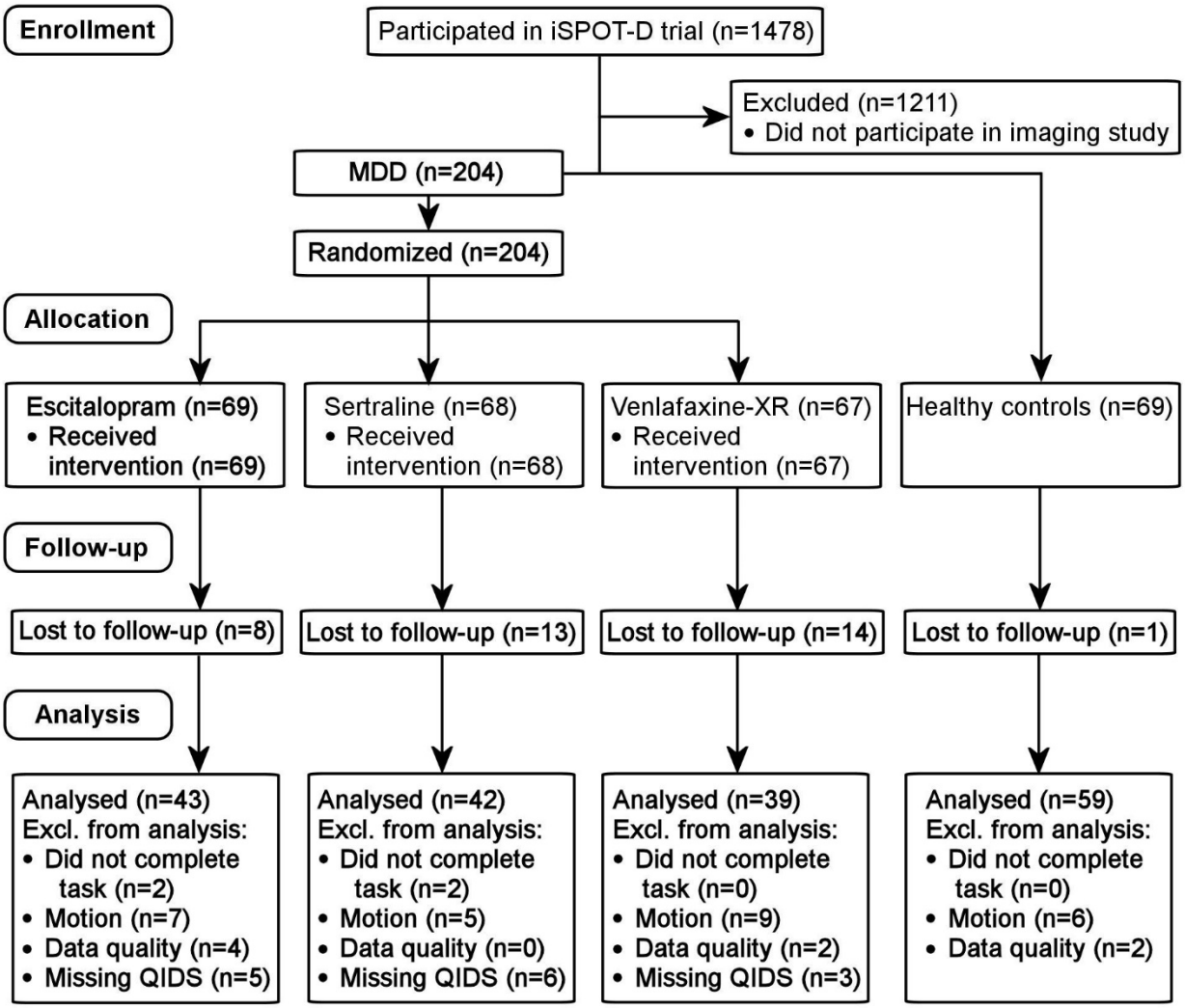

The original data was collected in the imaging arm of the international Study to Predict Optimized Treatment in Depression (iSPOT-D).

Abbreviations: Excl.=excluded, MDD=depressed patients, QIDS=Quick Inventory of Depressive Symptomatology scale, XR=extended release.

Figure S2: Overview of our Go-NoGo paradigm.

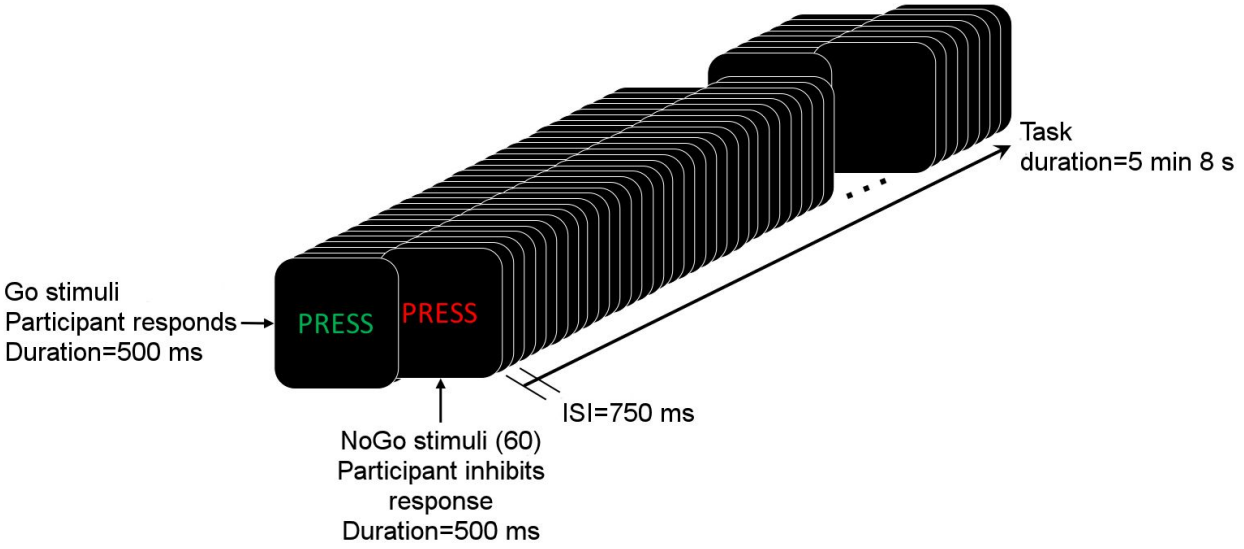

The paradigm comprised 60 NoGo stimuli (the word “press” in red) and 180 Go stimuli (the word “press” in green), presented one at a time in a pseudorandom sequence with a duration of 500 milliseconds and an interstimulus interval (ISI) of 0.75 seconds.

Figure S3: Results of the conjunction analysis for the activation during NoGo>Go in MDD and HC.

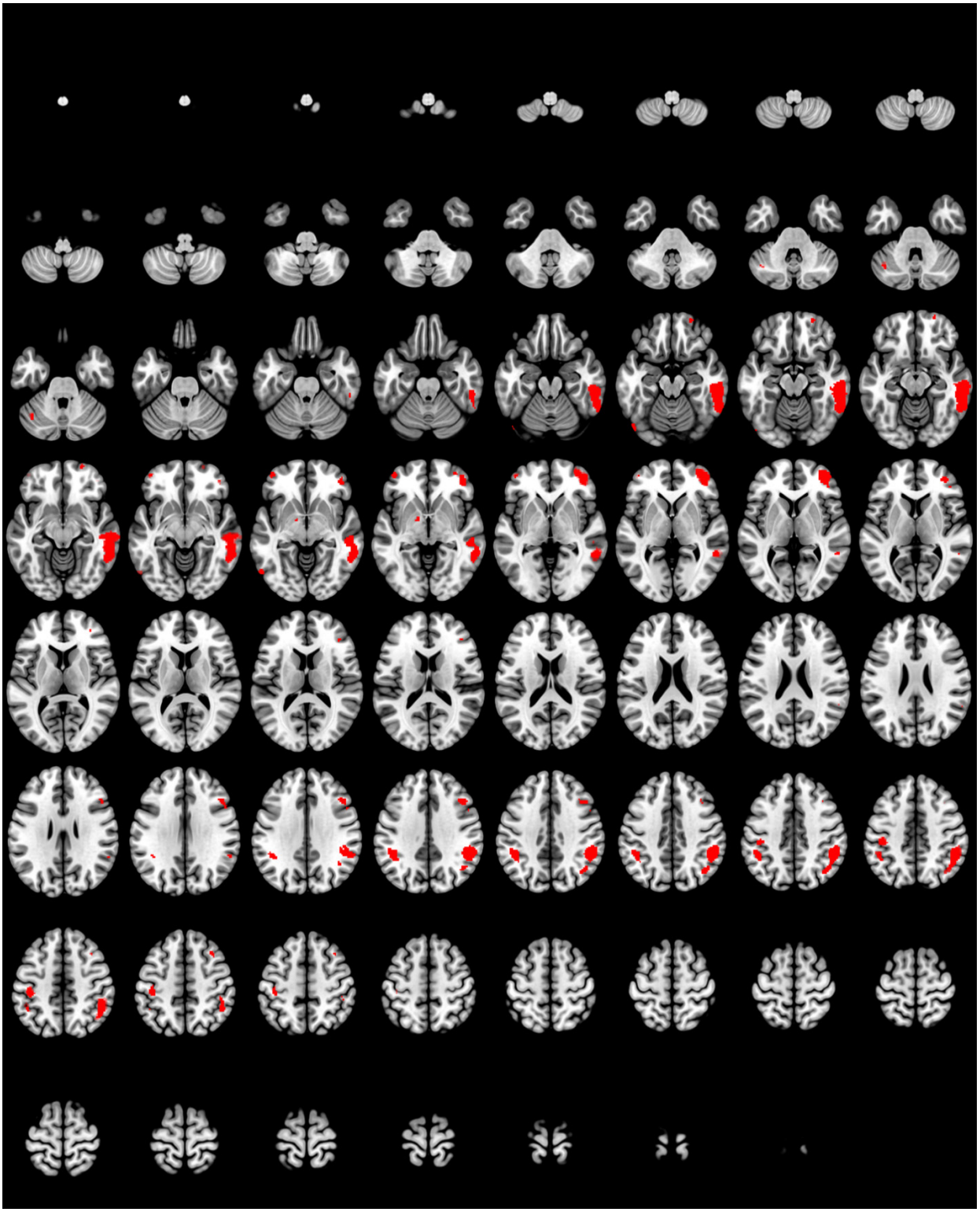

A one-sample t-test was computed in the two groups separately using the contrast maps from the first level (using age and sex as covariates). The ensuing maps were thresholded at whole-brain family-wise error (FWE) corrected $p<0.01$. Then, only voxels activated both in the HC and MDD were selected.

Abbreviations: HC=healthy controls, MDD=depressed patients.

Figure S4: ROIs of our gPPI analysis in relation to the activation clusters.

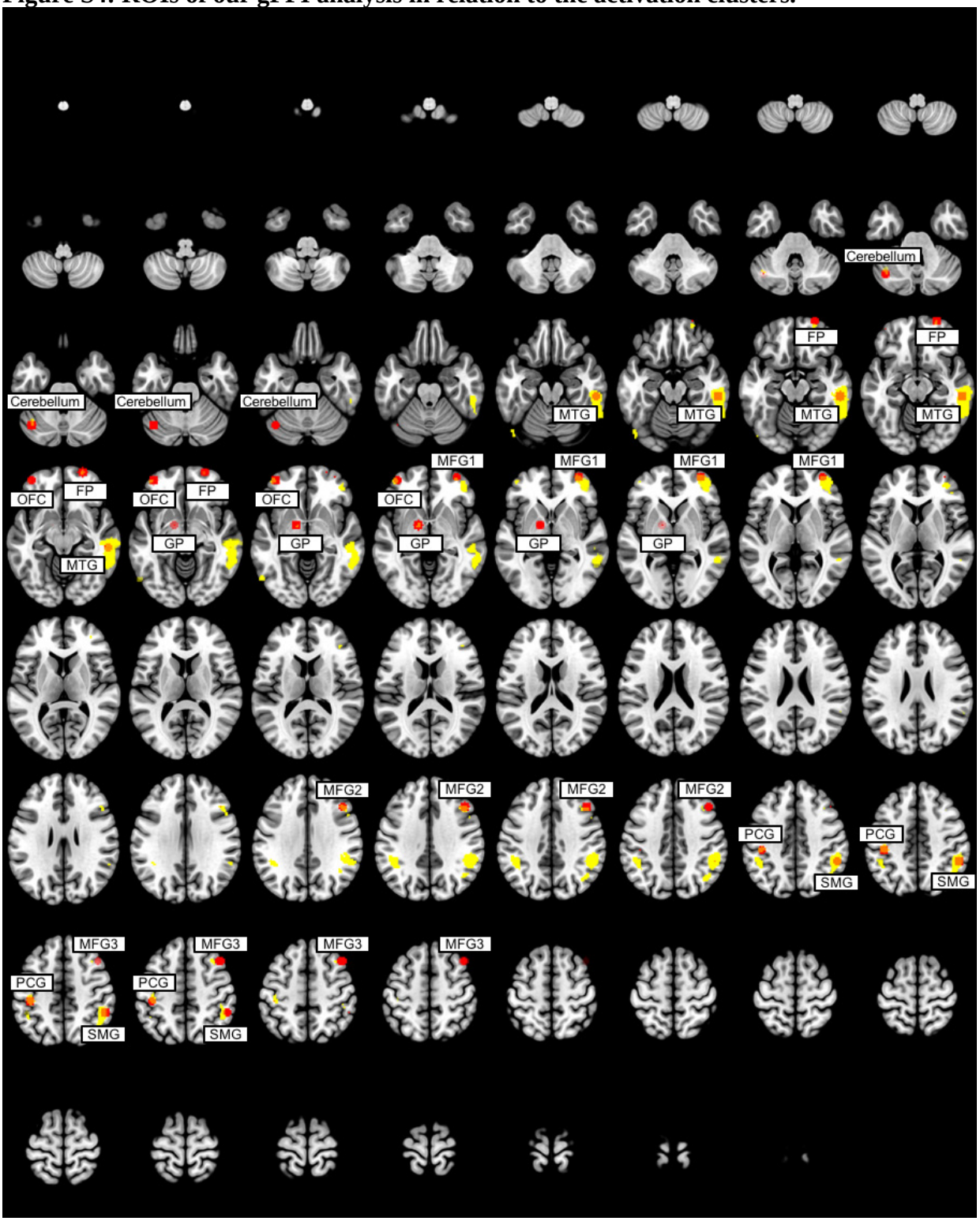

Spheres of 6 mm diameter (red) were built around the peak activations of the clusters presented in Figure S3 (yellow). Abbreviations match the ones reported in Table S3.

Abbreviations: FP=frontal pole, GP=globus pallidus, gPPI= generalized psychophysiological interaction toolbox, MFG=middle frontal gyrus, MTG=middle temporal gyrus, OFC=orbitofrontal cortex, PCG=postcentral gyrus, ROIs=regions of interest, SMG=supramarginal gyrus.

Figure S5: ROIs of our gPPI analysis in relation to meta-analysis results.

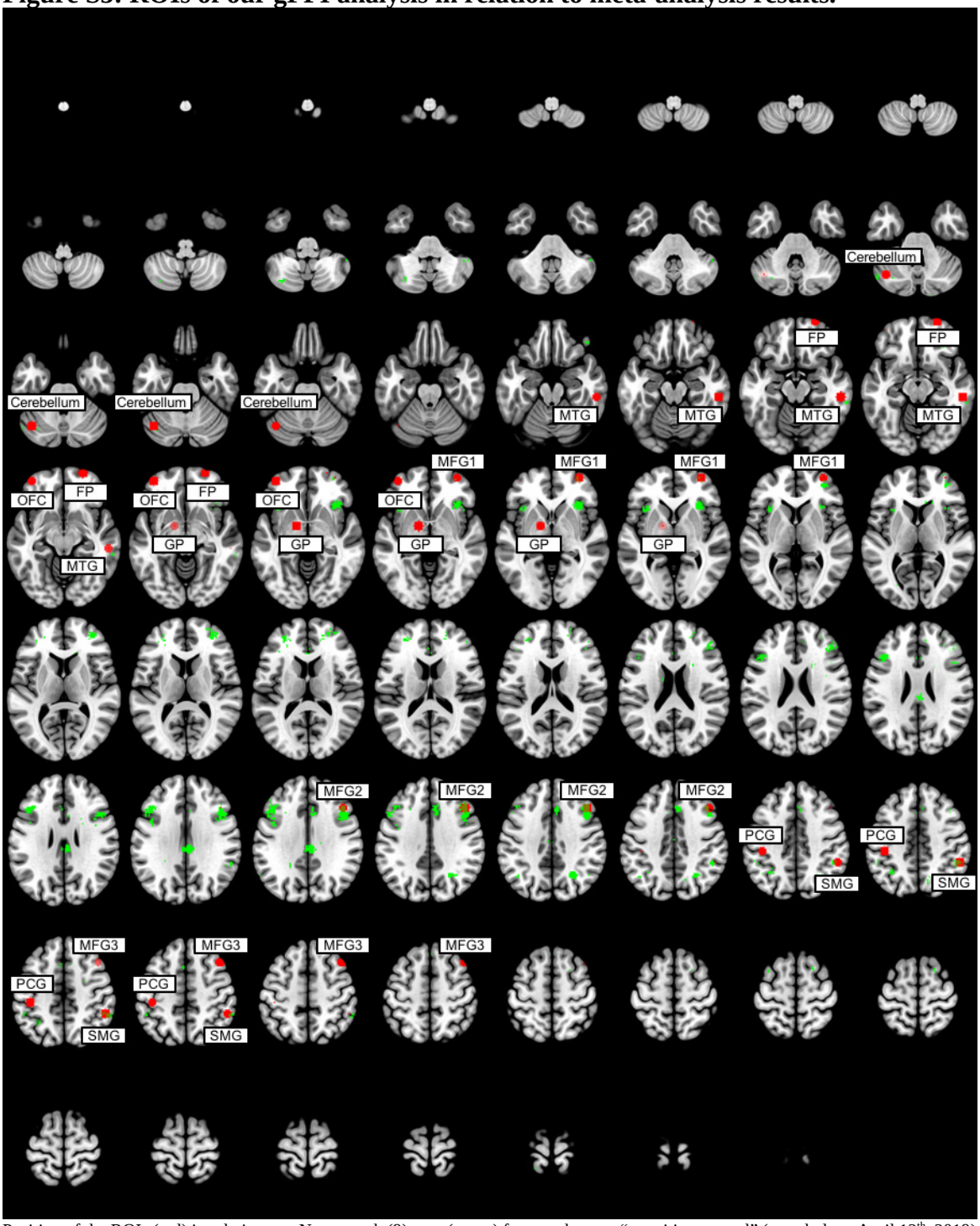

Position of the ROIs (red) in relation to a Neurosynth (9) map (green) for search term: "cognitive control" (search date: April 12th, 2019). Abbreviations match the ones reported in Table S3.

Abbreviations: FP=frontal pole, GP=globus pallidus, gPPI= generalized psychophysiological interaction toolbox, MFG=middle frontal gyrus, MTG=middle temporal gyrus, OFC=orbitofrontal cortex, PCG=postcentral gyrus, ROIs=regions of interest, SMG=supramarginal gyrus.

Figure S6: Results accounting for baseline QIDS-SR$_{16}$.

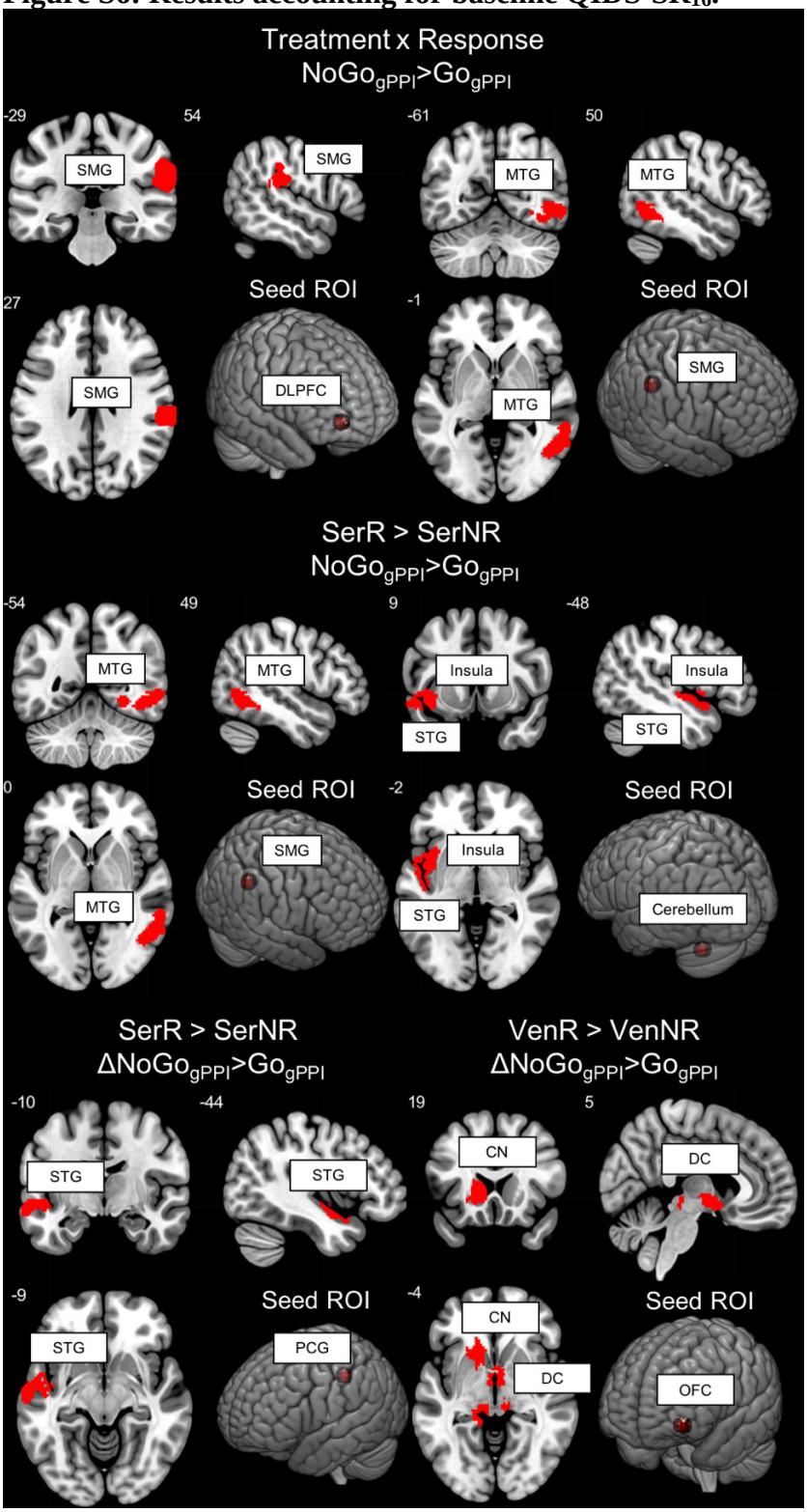

Main findings re-calculated with the addition of the baseline QIDS-SR$_{16}$ as a confound in the group level general linear models (in addition to age and sex). Compared to our original findings (Figures 1-3) the change was minimal.

Abbreviations: CN=caudate nucleus, gPPI=generalized psychophysiological interaction, DLPFC=dorsolateral prefrontal cortex, MTG=middle temporal gyrus, NR=non-responders, OFC=orbitofrontal cortex, PCG=postcentral gyrus, R=responders, ROI=region of interest, Ser=sertraline, SMG=supramarginal gyrus, STG=superior temporal gyrus, Ven=venlafaxine.

Figure S7: Connectivity between DLPFC and SMG for Go and NoGo trials.

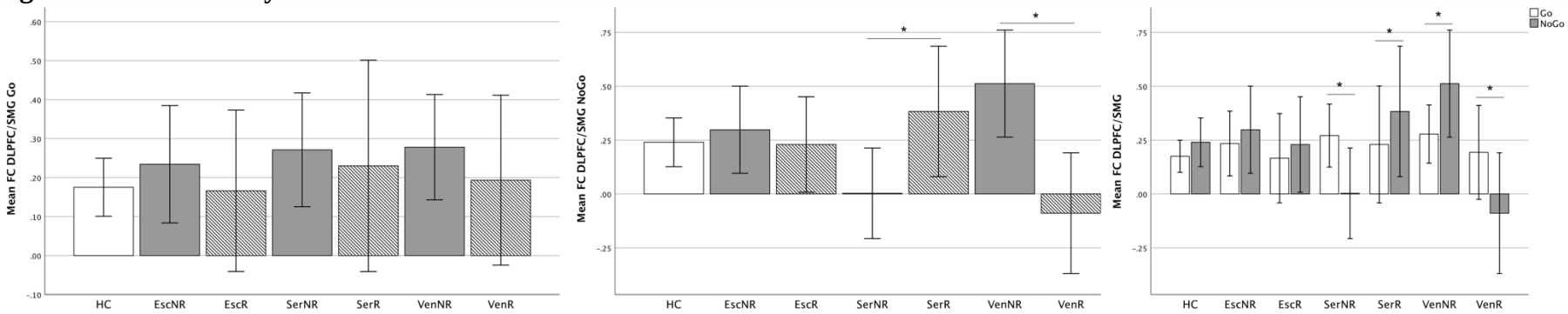

By comparing connectivity during the NoGo and Go conditions separately, we confirmed that the results of our interaction between treatment and response were driven by higher connectivity in responders during NoGo trials in the sertraline arm and lower in the venlafaxine arm. Stars mark significant comparisons between groups or within subject (t-test $p<0.05$). Bars represent 95% confidence intervals of the mean.

Abbreviations: DLPFC=dorsolateral prefrontal cortex (MFG1 in Table 2), Esc=escitalopram, FC=functional connectivity, HC=healthy controls, NR=non-responders, R=responders, Ser=sertraline, SMG=supramarginal gyrus, Ven=venlafaxine.

Figure S8: Connectivity between SMG and MTG for Go and NoGo trials.

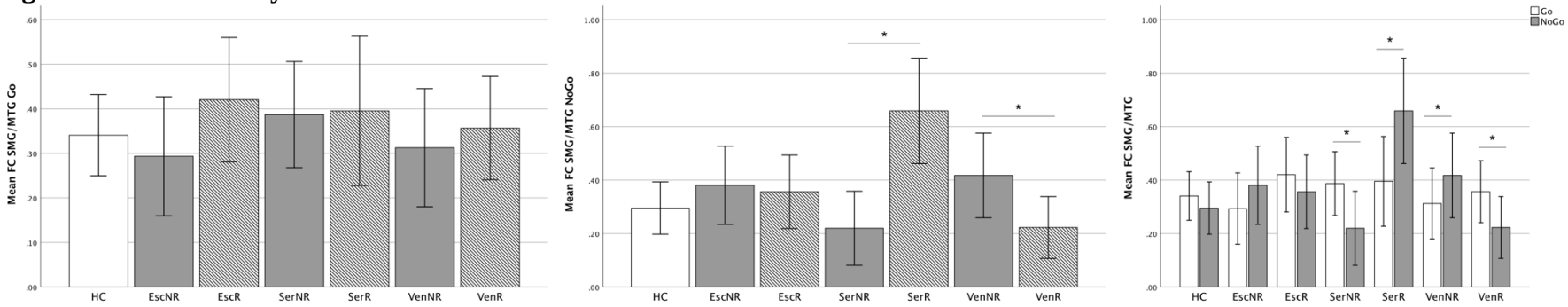

By comparing connectivity during the NoGo and Go conditions separately, we confirmed that the results of our interaction between treatment and response were driven by higher connectivity in responders during NoGo trials in the sertraline arm and lower in the venlafaxine arm. Stars mark significant comparisons between groups or within subject (t-test $p<0.05$). Bars represent 95% confidence intervals of the mean.

Abbreviations: Esc=escitalopram, FC=functional connectivity HC=healthy controls, MTG=middle temporal gyrus, NR=non-responders, R=responders, Ser=sertraline, SMG=supramarginal gyrus, Ven=venlafaxine.

Figure S9: Connectivity in the sertraline group for Go and NoGo trials.

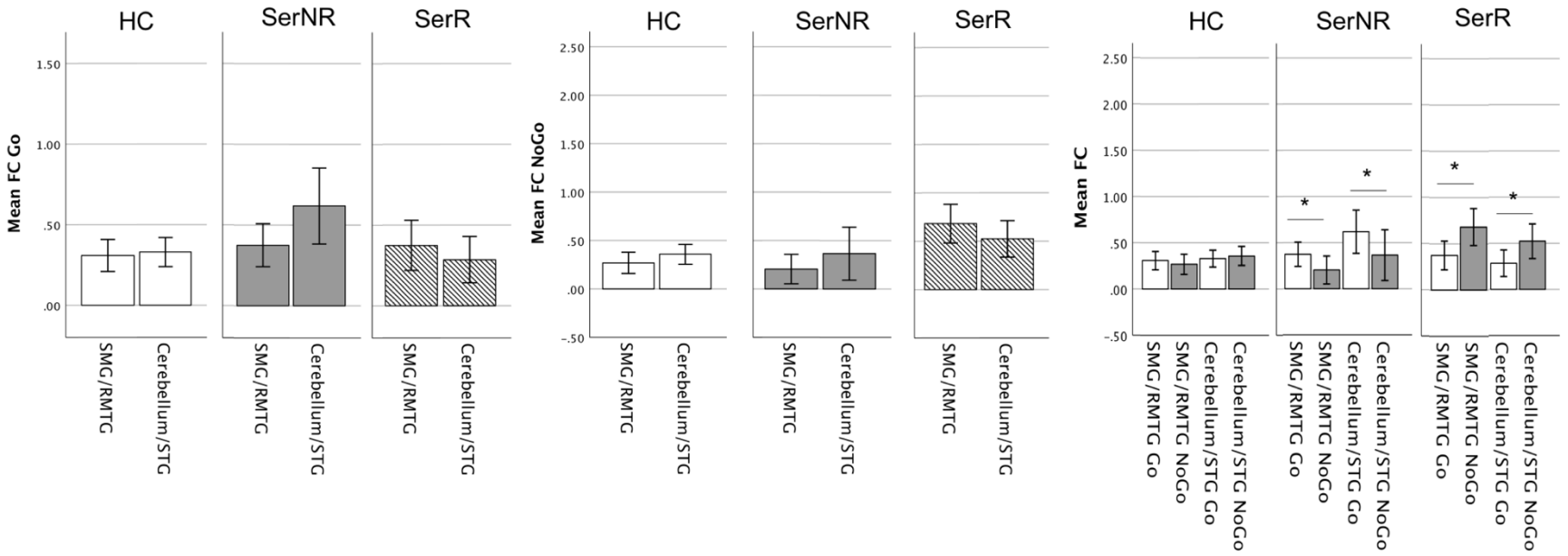

By comparing connectivity during the NoGo and Go conditions separately, we confirmed that the results of our interaction between treatment and response were driven by higher connectivity in responders during NoGo trials in the sertraline arm and lower in non-responders. Stars mark significant comparisons within subject (t-test $p<0.05$). Bars represent 95% confidence intervals of the mean.

Abbreviations: DLPFC=dorsolateral prefrontal cortex, FC=functional connectivity, HC=healthy controls, MTG=middle temporal gyrus, NR=non-responders, R=responders, Ser=sertraline, SMG=supramarginal gyrus, STG=superior temporal gyrus.

Figure S10: Longitudinal changes in connectivity in the sertraline group for Go and NoGo trials.

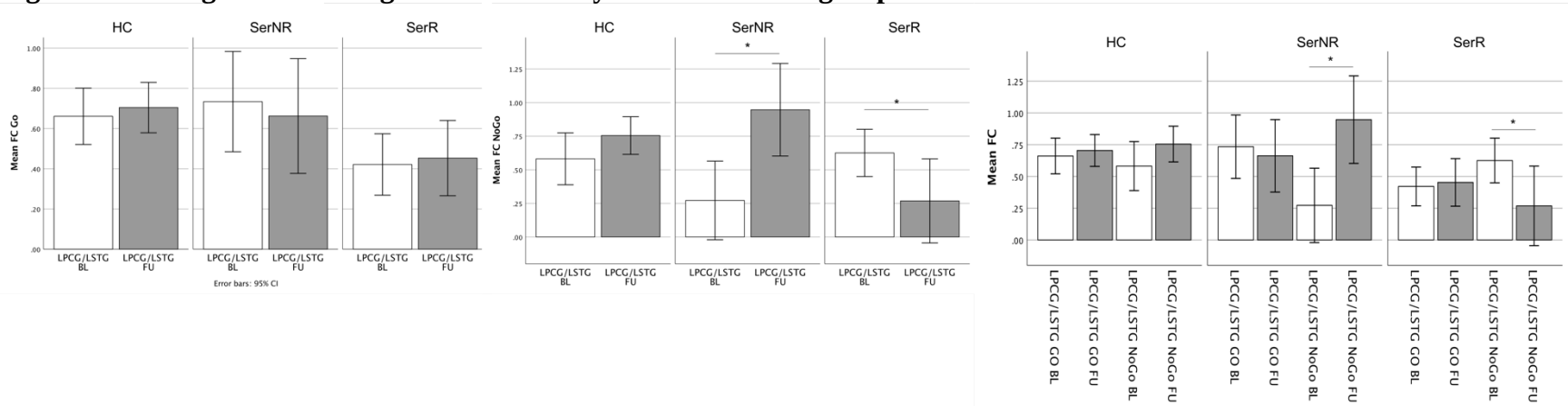

By comparing connectivity during the NoGo and Go conditions separately, we confirmed that the results of our changes following sertraline treatment were driven by a decrease of connectivity in responders during NoGo trials and an increase in non-responders. Stars mark significant comparisons within subject (t-test $p<0.05$). Bars represent 95% confidence intervals of the mean.

Abbreviations: BL=baseline, FC=functional connectivity, FU=follow-up, HC=healthy controls, L=left, PCG=precentral gyrus, NR=non-responders, R=responders, Ser=sertraline, STG=superior temporal gyrus.

Figure S11: Longitudinal changes in connectivity in the venlafaxine group for Go and NoGo trials.

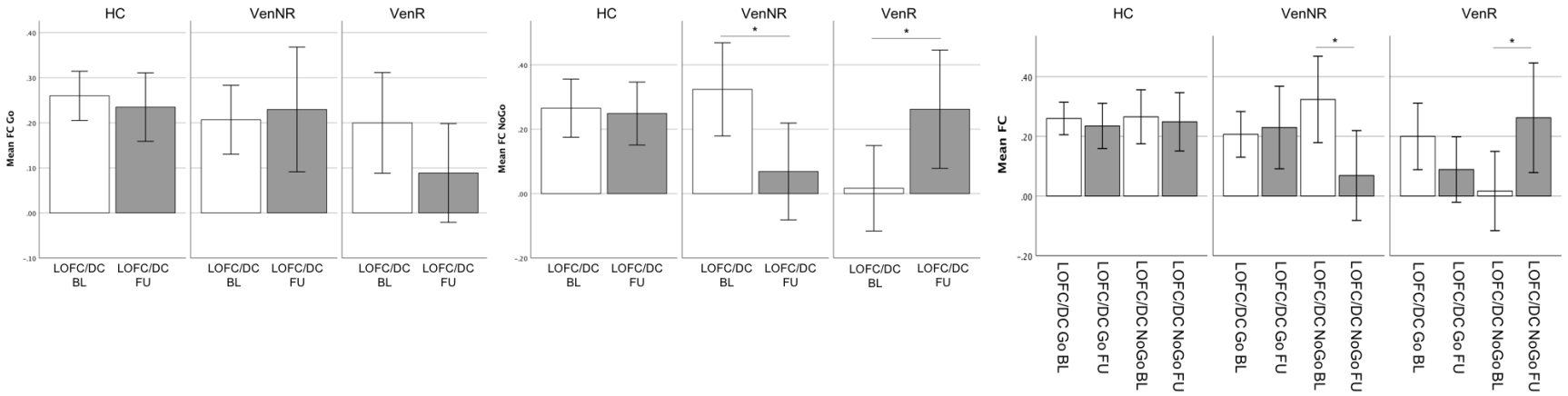

By comparing connectivity during the NoGo and Go conditions separately, we confirmed that the results of our changes following venlafaxine treatment were driven by an increase of connectivity in responders during NoGo trials and a decrease in non-responders. Stars mark significant comparisons within subject (t-test $p<0.05$). Bars represent 95% confidence intervals of the mean.

Abbreviations: BL=baseline, DC=diencephalon, FC=functional connectivity, FU=follow-up, HC=healthy controls, L=left, NR=non-responders, OFC=orbital frontal cortex, R=responders, Ven=venlafaxine

Figure S12: Connectivity of the DLPFC and supramarginal gyrus in relationship to resting state networks.

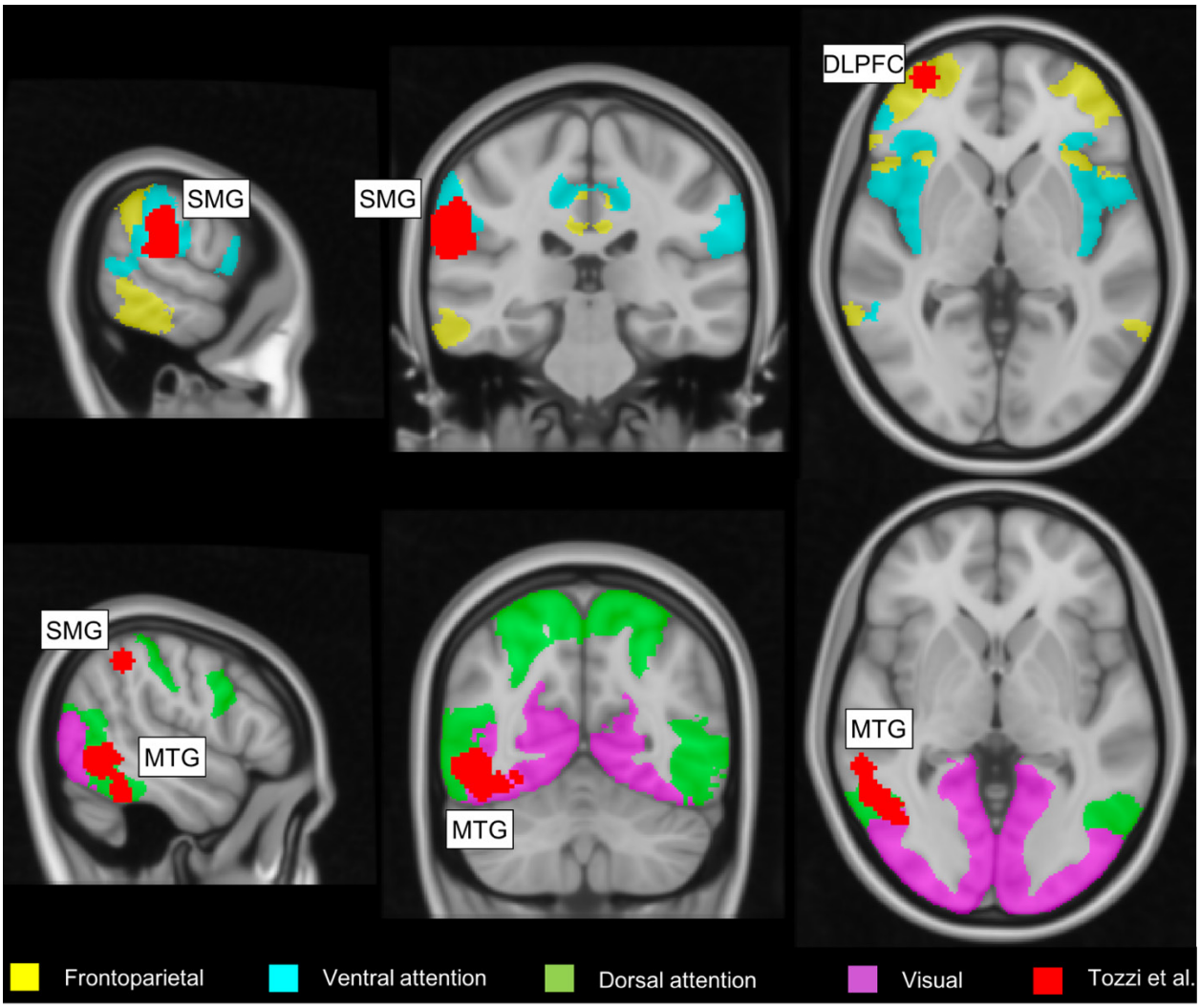

We show the location of our findings (red) predicting differential treatment response to sertraline and venlafaxine (see Figure 1 in main text) in relationship with known resting state functional networks as defined by Yeo et al. (11). Responders to sertraline showed higher functional connectivity between the DLPFC and supramarginal gyrus and between supramarginal gyrus and middle temporal gyrus compared to non-responders, whereas in the venlafaxine group the opposite was true.

Abbreviations: DLPFC=dorsolateral prefrontal cortex, MTG=middle temporal gyrus, SMG=supramarginal gyrus.

Figure S13: Connectivity of the SMG and cerebellum in relationship to resting state networks.

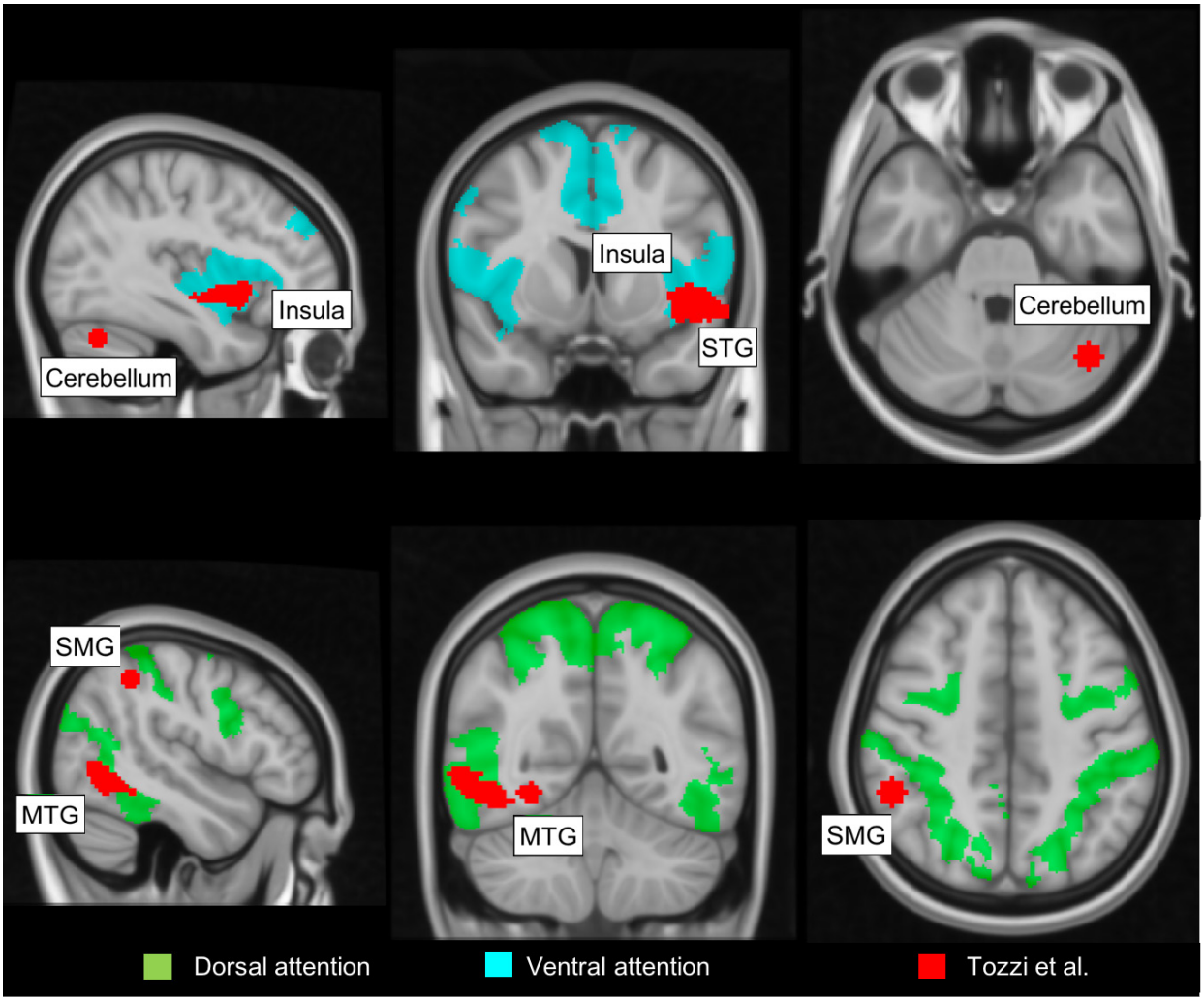

We show the location of our findings (red) predicting differential treatment response to sertraline (see Figure 2 in main text) in relationship with known resting state functional networks as defined by Yeo et al. (11). Responders to sertraline showed higher functional connectivity between the cerebellum, superior temporal gyrus and insula as well as between the supramarginal gyrus and right middle temporal gyrus compared to non-responders.

Abbreviations: MTG=middle temporal gyrus, SMG=supramarginal gyrus, STG=superior temporal gyrus.

Figure S14: Connectivity correlates of antidepressant response in relationship to resting state networks.

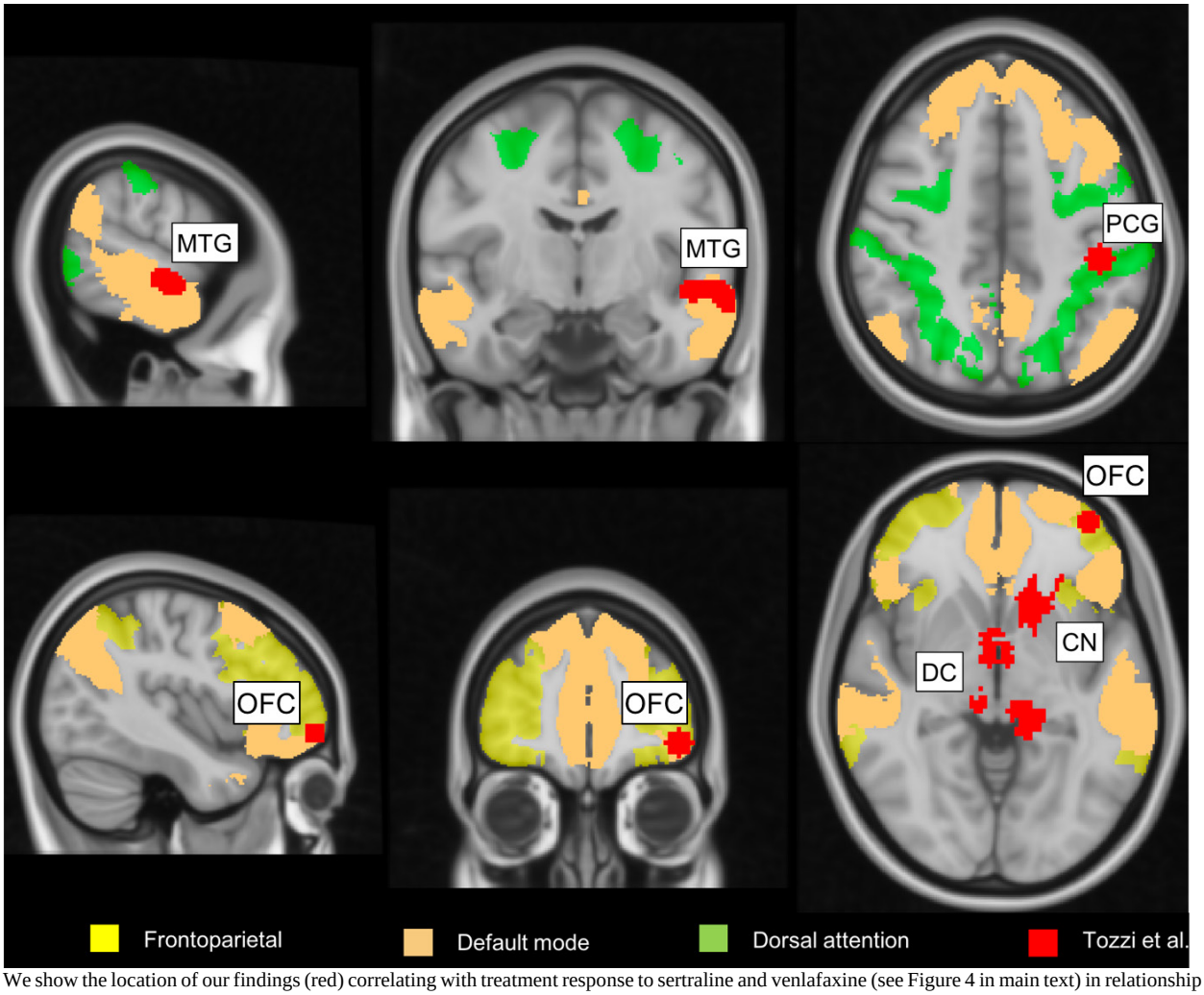

We show the location of our findings (red) correlating with treatment response to sertraline and venlafaxine (see Figure 4 in main text) in relationship with known resting state functional networks as defined by Yeo et al. (11). Responders to sertraline showed a decrease in functional connectivity between the postcentral gyrus and superior temporal gyrus, whereas non-responders showed an increase. Responders to venlafaxine showed a decrease in functional connectivity between the orbitofrontal cortex, the diencephalon and caudate nucleus.

Abbreviations: CN=caudate nucleus, DC=diencephalon, MTG=middle temporal gyrus, OFC=orbitofrontal cortex, PCG=postcentral gyrus.

Supplemental References

1. Power JD, Mitra A, Laumann TO, Snyder AZ, Schlaggar BL, Petersen SE (2014): Methods to detect, characterize, and remove motion artifact in resting state fMRI. *NeuroImage*. 84: 320–341.

2. Siegel JS, Power JD, Dubis JW, Vogel AC, Church JA, Schlaggar BL, Petersen SE (2014): Statistical improvements in functional magnetic resonance imaging analyses produced by censoring high-motion data points. *Hum Brain Mapp*. 35: 1981–1996.

3. Power JD, Barnes KA, Snyder AZ, Schlaggar BL, Petersen SE (2012): Spurious but systematic correlations in functional connectivity MRI networks arise from subject motion. *NeuroImage*. 59: 2142–2154.

4. McLaren DG, Ries ML, Xu G, Johnson SC (2012): A generalized form of context-dependent psychophysiological interactions (gPPI): a comparison to standard approaches. *Neuroimage*. 61: 1277–1286.

5. Langenecker SA, Kennedy SE, Guidotti LM, Briceno EM, Own LS, Hooven T, *et al.* (2007): Frontal and limbic activation during inhibitory control predicts treatment response in major depressive disorder. *Biol Psychiatry*. 62: 1272–1280.

6. Gyurak A, Patenaude B, Korgaonkar MS, Grieve SM, Williams LM, Etkin A (2016): Frontoparietal activation during response inhibition predicts remission to antidepressants in patients with major depression. *Biol Psychiatry*. 79: 274–281.

7. Tong Y, Chen Q, Nichols TE, Rasetti R, Callicott JH, Berman KF, *et al.* (2016): Seeking Optimal Region-Of-Interest (ROI) Single-Value Summary Measures for fMRI Studies in Imaging Genetics. *PLOS ONE*. 11: e0151391.

8. Chumbley J, Worsley K, Flandin G, Friston K (2010): Topological FDR for neuroimaging. *NeuroImage*. 49: 3057–3064.

9. Yarkoni T, Poldrack RA, Nichols TE, Van Essen DC, Wager TD (2011): Large-scale automated synthesis of human functional neuroimaging data. *Nat Methods*. 8: 665–670.

10. Varma S, Simon R (2006): Bias in error estimation when using cross-validation for model selection. *BMC Bioinformatics*. 7: 91.

11. Thomas Yeo BT, Krienen FM, Sepulcre J, Sabuncu MR, Lashkari D, Hollinshead M, *et al.* (2011): The organization of the human cerebral cortex estimated by intrinsic functional connectivity. *J Neurophysiol*. 106: 1125–1165.